Surface-Initiated Ring-Opening Metathesis Polymerization (SI-ROMP): Synthesis and Electropolymerization of Terthiophene-Functionalized Olefin Peripheral Dendrons

ARTICLE *in* MACROMOLECULES · NOVEMBER 2010

Impact Factor: 5.8 · DOI: 10.1021/ma101746e

5 AUTHORS, INCLUDING:

Roderick B Pernites
University of Houston
29 PUBLICATIONS **535** CITATIONS
SEE PROFILE

Rigoberto C. Advincula
Case Western Reserve University
332 PUBLICATIONS **7,208** CITATIONS
SEE PROFILE

10262 *Macromolecules* **2010**, *43*, 10262–10274
DOI: 10.1021/ma101746e

Macromolecules
ARTICLE

Surface-Initiated Ring-Opening Metathesis Polymerization (SI-ROMP): Synthesis and Electropolymerization of Terthiophene-Functionalized Olefin Peripheral Dendrons

Guoqian Jiang, Ramakrishna Ponnapati, Roderick Pernites, Mary Jane Felipe, and Rigoberto Advincula*

Department of Chemistry and Department of Chemical and Biomolecular Engineering, University of Houston, Houston, Texas 77204-5003, United States

Received July 31, 2010; Revised Manuscript Received October 30, 2010

ABSTRACT: We report on the synthesis and electrodeposition of peripheral olefin dendrons with electropolymerizable focal point terthiophene units. These films were utilized for surface initiated ring-opening metathesis polymerization (SI-ROMP) of norbornene to form grafted polynorbornene brushes. The dendrons were first electrodeposited on an electrode surface, forming a highly dense and uniform polythiophene-type film, and their electrochemical behavior was investigated. Subsequently, after activation with a transition metal metathesis catalyst, polynorbornene brushes were grown from the electrodeposited films which were found to be highly dependent on the density of exposed olefin functional groups and dendron generation. The change in film morphology was examined by atomic force microscopy (AFM). X-ray photoelectron spectroscopy (XPS) was used to prove polynorbornene brush film growth and composition on top of the electropolymerized layer. Brush growth kinetics experiments were also carried out to understand the correlation between the structure of the dendrons and polynorbornene brush growth mechanism. The method presented in this paper provides a facile route to prepare robust, uniform, and controllable polymer brushes grafted from an underlying π-conjugated polymer layer.

1. Introduction

Polymer brushes via surface-initiated polymerization (SIP) on flat surfaces and colloidal particles have received much interest because of their synthetic inimitability.[1] There are, in general, two different approaches—"grafting to" and "grafting from"—to grow polymer brushes. Compared to the "grafting to" method which usually results in nonuniform films with low surface coverage, slow grafting, and poor adhesion, the "grafting from" approach or SIP allows monomers of interest to controllably grow from surface-bound initiators. Therefore, the properties of brush films generated by SIP can be modified by varying parameters related to the type of initiation mechanism, grafting density, and control on degree of polymerization.[2] The surface initiators, in most cases, are covalently attached to surfaces via self-assembled monolayers (SAMs). This provides a uniform surface coverage of the initiating functional groups with the possibility for obtaining block copolymers or mixed polymer brush systems.

Surface-initiated ring-opening metathesis polymerization (SI-ROMP) has emerged as a novel method to synthesize polymer brushes using late transition metal catalysts.[3] As a living/controlled polymerization technique, SI-ROMP offers the capability of preparing uniform polymer brushes and block copolymers by metathesis methods. In addition, it has shown rapid reaction kinetics under mild conditions. Jennings et al. recently investigated SI-ROMP kinetics by varying the alkyl chain length on the side of norbornene monomers.[4] Different functional groups have been introduced into norbornene monomers to form polymer brushes for a variety of applications. For example, photochromic polymer brushes have been reported by Locklin et al. based on photoinduced isomerization of spiropyran-functionalized polynorbornene films.[5] Choi and co-workers have reported the formation of diblock copolymer brushes via SI-ROMP and their morphological changes upon exposure to different solvents.[6]

In the immobilization of surface initiators onto flat electrically conductive substrates, the formation of SAMs from silane or thiol molecules provides two-dimensionally ordered surfaces for polymer brush growth. Besides SAMs, different strategies have been developed to prepare polymer layers on conductive surfaces.[7−13] Electrochemical deposition of polyacrylate films provides a sublayer which includes active surface initiators. The polymer brushes are then chemically attached to the conducting electrode surface.[8−10] Detrembleur et al. combined electrografting and ROMP to prepare polynorbornene brushes on conductive substrates.[14] In their work, they first electrochemically grafted poly(norbornenylmethylene acrylate) films which were activated by Grubbs catalyst on the norbornenyl pendant groups. Then a SI-ROMP procedure of norbornene monomer generated poly(norbornene-*co*-acrylate) brush films with several micrometers in thickness. However, this strategy usually yields only thin initiator-containing polymer films due to rapid passivation of the cathode by the insulating polyacrylate layer and early termination of polymerization. Moreover, in the cathodic electropolymerization process, monomers containing protic functional groups such as alcohol, amine, and carboxylic acid cannot be electrografted due to their reduction at the same or at a less cathodic potential than the (meth)acrylate. Relatively anodic polymerization of monomers bearing surface initiating functionalities is more facile and controllable over a wider range of solvents.

Herein, we report a new method to attach ROMP surface initiators onto electrode surfaces by electrochemically depositing a polythiophene film with different generations of dendritic peripheral olefin functional groups (Scheme 1). From a statistical point of view, there should be a controlled number of free

*To whom correspondence should be addressed. E-mail: radvincula@uh.edu.

 Published on Web 11/24/2010

Scheme 1. Electrochemical Deposition of Frechet-Type Peripheral Olefin Dendrons Leading to a Dendronized Polythiophene[a]

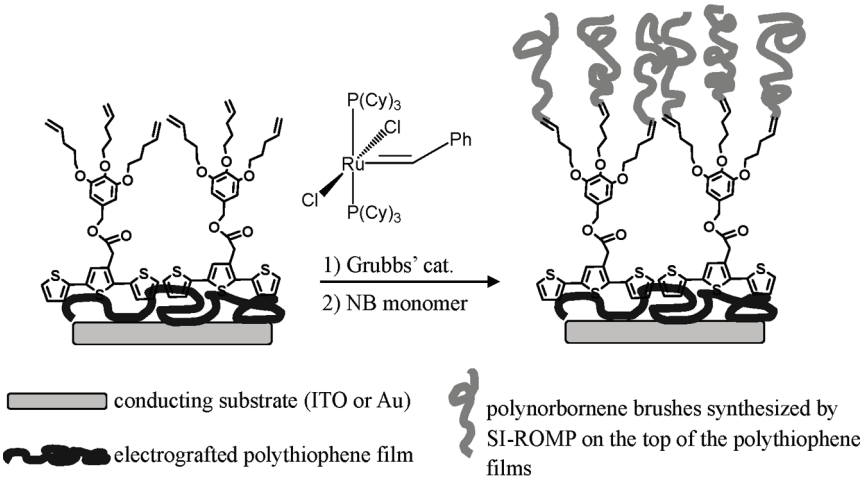

[a] This is followed by SI-ROMP of norbornene on the eletropolymerized films. Shown below the diagram is a possible polymer structure for a G1 thiophene dendron with three olefin groups.

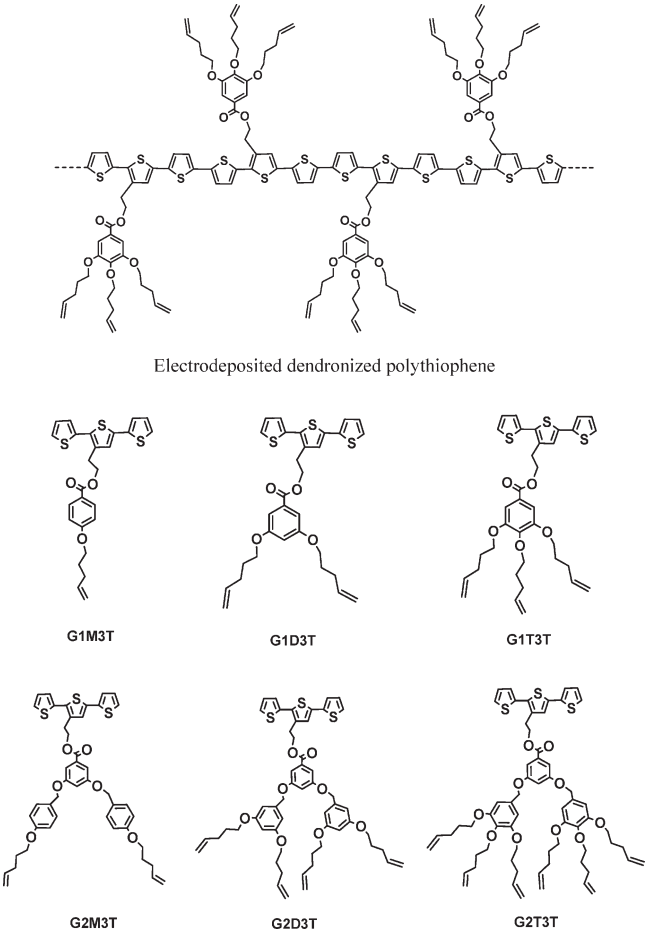

Figure 1. First and second generations of the Frechet-type olefin dendrons with terthiophene at the focal point used in this study and the varying number of olefinic peripheral groups. Here we define "G1/G2" as the first/second generation, "M/D/T" as the mono/di/trisubstituted olefin side chains, and "3T" as terthiophene. For example, G1M3T represents the first generation (G1) dendron with the monosubstituted (M) olefin functional group as the pendant and the terthiophene (3T) group as the focal point.

olefin functional groups available for Grubbs' catalyst activation. Polymer brush density will therefore be highly dependent on the population of activated olefins. In this regard, we synthesized a series of generational Frechet-type peripheral olefin dendrons with terthiophene at the focal point as shown in Figure 1. By cyclic voltammetry (CV), the polymerization of the terthiophene-containing dendron molecules leads to the deposition of polythiophene films onto the electrodes. By this anodic electrochemical polymerization method involving radical cations, polythiophene films can be continuously deposited without significant passivation of the electrodes. Thus, it is possible to achieve high density of free olefins as well as generate an electrically conducting polymer sublayer. Generation 1 and 2 of these dendritic molecules were synthesized with a range of 1−6 olefinic groups based on a branched phenyl and benzyl ether functionality (Figure 1) in an attempt to correlate their number with electrochemical behavior and outcome in a SI-ROMP procedure. Polynorbornene as the model brush film was then grown from the electropolymerized films after activation by the first-generation Grubbs catalyst, as shown in Scheme 1. Ellipsometric measurements were first carried out to track the polymer film growth ex situ. Polymer growth kinetics was then investigated by measuring the polymer brush film thickness as a function of polymerization time. X-ray photoelectron spectroscopy (XPS) was used to investigate film composition. Atomic force microscopy (AFM) was used to examine morphology changes before and after SI-ROMP.

This method is seemingly more complicated, as compared to the normal method which introduces surface initiators from SAMs. However, SAMs are typically compatible only with specific metal or nonmetal substrates. The restricted two-dimensional arrangement also limits the conformational freedom and accessibility of the functional groups on the surface. Our group has recently reported the preparation of protein and cell-resistant poly(polyethylene glycol methyl ether methacrylate) (PPEGMEMA) brushes by surface-initiated reversible addition−fragmentation chain transfer (SI-RAFT) polymerization. The process started with the electrochemical deposition of an electroactive chain transfer agent (CTA) including carbazole units on the Au surface, which serves as the surface initiating layer.[15] In our present paper, we aim to not only extend this idea to SI-ROMP but also illustrate how the electroactive dendron structure and electropolymerization conditions affect the subsequent polymer brush growth.

2. Experimental Section

2.1. Materials. Reagent chemicals were purchased from Sigma-Aldrich, VWR, Alfa Aesar, or Acros Organics and used without further purification unless otherwise indicated. Tetrahydrofuran (THF) used in synthesis was distilled from sodium/benzophenone

Scheme 2. Synthesis of the Monosubstituted Terminal Olefin Dendrons (G1M3T and G2M3T) with Electropolymerizable Terthiophenes at the Focal Points

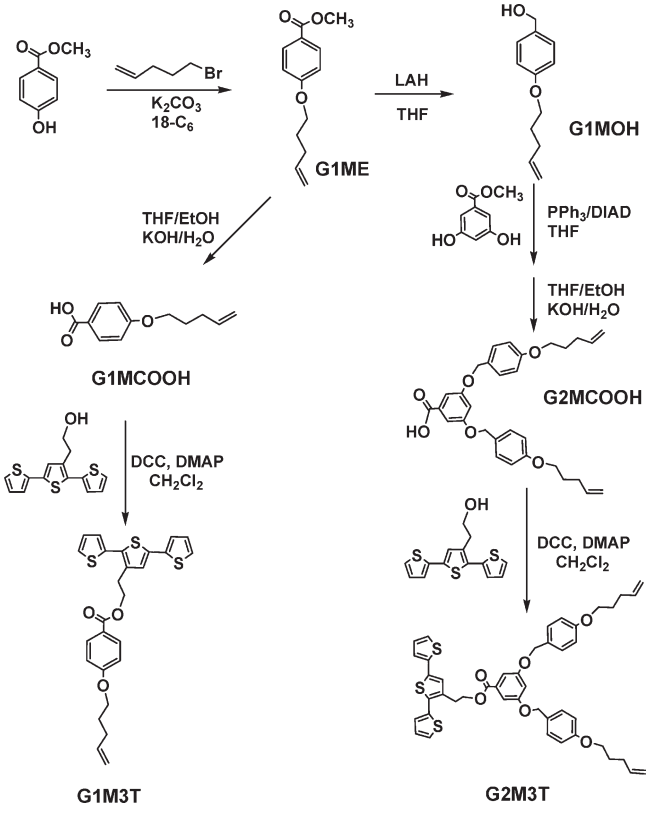

Scheme 3. Synthesis of the Disubstituted Terminal Olefin Dendrons (G1D3T and G2D3T) with Electropolymerizable Terthiophenes at the Focal Points

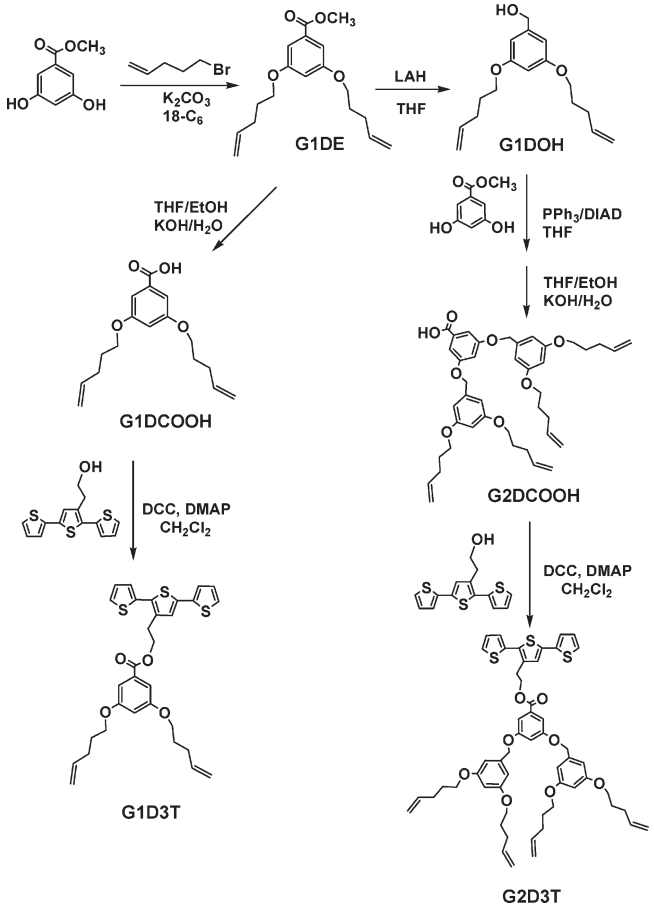

ketyl. Methylene chloride (CH_2Cl_2) used in synthesis was distilled from CaH_2. Grubbs first-generation catalyst was purchased from Aldrich and used as received. Carbazole-containing alkylthiol and alkylsilane were synthesized according to previous reports.[16,17]

2.2. Instrumentation. Nuclear magnetic resonance (NMR) spectra were recorded on a General Electric QE-300 spectrometer at 300 MHz for ^1H NMR. The electropolymerization of the dendron molecules was carried out on a Princeton Applied Research Parstat 2263. Carbazole-SAM-covered indium tin oxide (ITO) or gold substrates were used as working electrodes coupled with a Pt wire as counter electrode and Ag/AgCl wire as reference electrode. The gold-coated thin film (~150 nm) substrates were prepared from thermoevaporation on glass or silicon wafer slides under high vacuum ($<5 \times 10^{-7}$ Torr). The ITO substrates were pretreated with the RCA recipe ($H_2O/H_2O_2/NH_3$::15.1 g/26.6 g/8.57 g). Cyclic voltammetry (CV) was utilized to prepare the polythiophene films from a 5 mM solution of the dendrons in 0.1 M $TBAPF_6/CH_3CN$, where $TBAPF_6$ is tetrabutylammonium hexafluorophosphate. For all the measurements, the electrode area exposed to the supporting electrolyte solution is 0.785 cm^2. The surface morphology of the electropolymerized films and the polymer brush films were examined by tapping mode AFM [PicoPlus System, Molecular Imaging (now Agilent Technologies), Tempe, AZ] under ambient conditions (24 °C and ~55% relative humidity). All image processing was performed using the SPIP software (Scanning Probe Image Processor, Image Metrology). XPS was carried out on a Physical Electronics 5700 instrument with photoelectrons generated by the nonmonochromatic Al Kα irradiation (1486.6 eV). Photoelectrons were collected at a takeoff angle of 45° using a hemispherical analyzer operated in the fixed retard ratio mode with an energy resolution setting of 11.75 eV. The binding energy scale was calibrated prior to analysis using $Cu^{2p_{3/2}}$ and $Ag^{3d_{5/2}}$ lines. Charge neutralization was ensured through cobombardment of the irradiated area with an e-beam using nonmonochromated Al Kα source and placing the C^{1s} peak at a binding energy of 284.6 (0.2) eV.

2.3. Synthesis of the Peripheral Olefin Dendrons. The details of the synthesis protocols are outlined below, and the synthesis routes are outlined in Schemes 2, 3, and 4.

2.3.1. General Synthesis Procedure for Etherification. To a suspension of methyl benzoate with each of the different hydroxyl-substituted phenyl groups (mono-, di-, and trisubstituted), potassium carbonate, and 18-crown-6 ether in acetone was added 5-bromopentene dropwise under continuous stirring. The suspension was then refluxed for 48 h. Acetone was evaporated under vacuum, and the residue was washed between water and CH_2Cl_2. The organic layer was separated, and the aqueous layer was extracted three times with CH_2Cl_2. Finally, the organic layer was combined and dried over anhydrous Na_2SO_4. After removal of the solvent, the crude product was purified by a silica gel column chromatography using pure CH_2Cl_2 as the eluent.

2.3.2. General Synthesis Procedure for Reduction by LAH. To a suspension of lithium aluminum hydride (LAH) in THF precooled to 0 °C was added a THF solution of the esters dropwise through a funnel. Once the addition was complete, the solution was allowed to stir for another 5 min and then warmed to room temperature and stirred for 24 h. The reaction was quenched by the addition of water. The pH of the reaction mixture was then adjusted with 2 M aqueous HCl to ~7.0. The solvent was evaporated under vacuum. The residue solution was extracted with CH_2Cl_2, and each organic layer was washed with an equal volume of water. The combined organic layers were dried over Na_2SO_4, filtered, and evaporated.

2.3.3. General Synthesis Procedure for Mitsunobu Coupling. The Mitsunobu etherification was carried out under sonication in order to expedite the reaction according to a previous report.[18] The mixture of alcohol, phenol, and triphenylphosphine (PPh_3)

Scheme 4. Synthesis of the Trisubstituted Terminal Olefin Dendrons (G1T3T and G2T3T) with Electropolymerizable Terthiophenes at the Focal Points

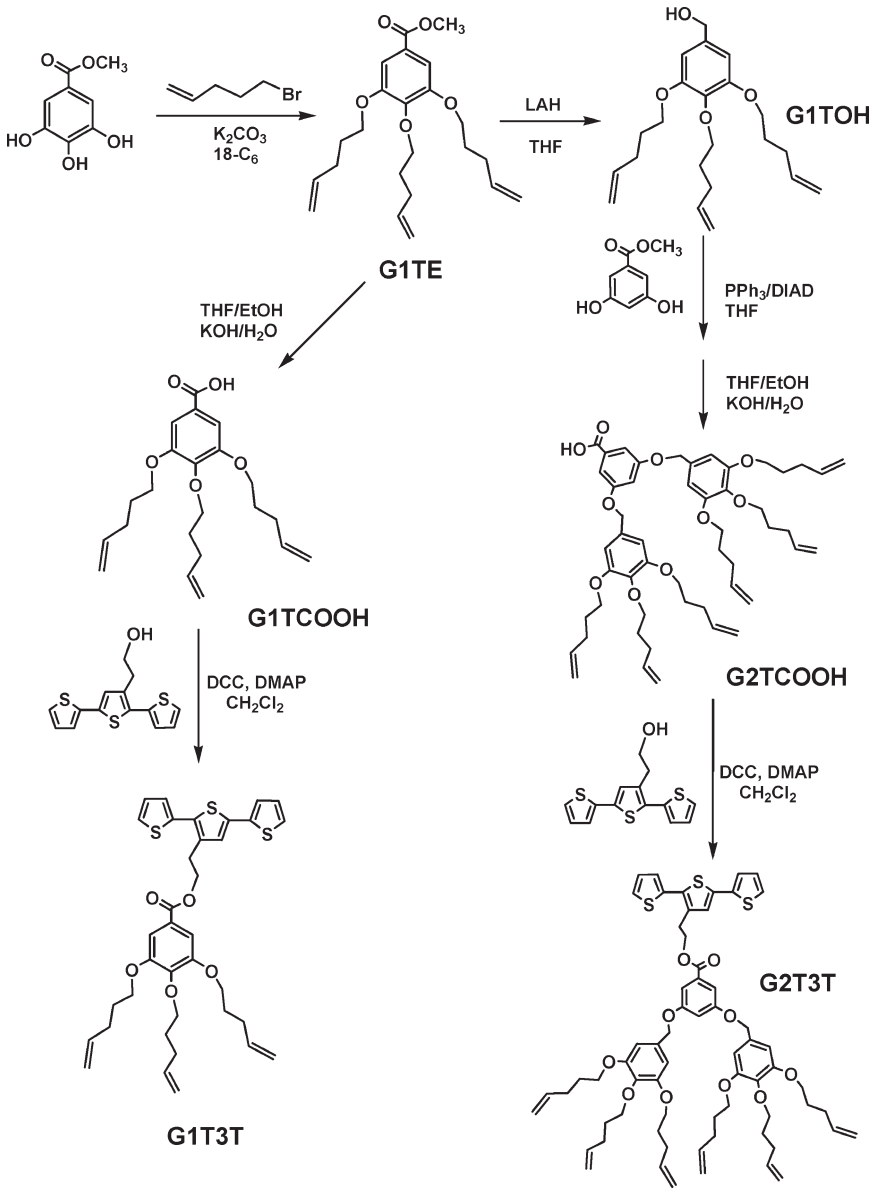

in minimal THF was cooled to 5 °C in an ice−water bath and sonicated for 10 min. Under sonication, a solution of diisopropyl azodicarboxylate (DIAD) was added dropwise through a syringe under the protection of nitrogen. The water temperature was allowed to warm to room temperature, and precautions were taken to maintain the temperature. (*Caution*: water in the sonicator turns very hot if sonicated for a long time.) The reaction was quenched by adding water, and the THF was removed by vacuum evaporation. The aqueous layer was extracted with CH_2Cl_2, and each organic layer was washed with dilute KOH solution and an equal volume of water. The product was purified using 4:1 CH_2Cl_2/hexane as an eluent by silica gel column chromatography.

2.3.4. General Synthesis Procedure of Hydrolysis. A solution of methyl benzoate ester in THF was mixed with ethanol. Saturated KOH aqueous solution was then added under vigorous stirring. The mixture was refluxed at 80 °C under a nitrogen atmosphere for 24 h. THF and EtOH were then removed under vacuum evaporation. The residue was diluted with water and the pH adjusted to 3 with a concentrated HCl solution. The solution was washed with CH_2Cl_2 and water. The organic layers were combined, dried over Na_2SO_4, filtered, and evaporated.

2.3.5. General Synthesis Procedure for Esterification. A solution of terthiophene alcohol (3TOH) was synthesized according to an earlier report;[19] terminal olefin dendron carboxylic acid and *p*-(dimethylamino)pyridine (DMAP) in anhydrous CH_2Cl_2 were kept stirring at 0 °C in an ice−water bath under a nitrogen atmosphere for 15 min. Dicyclohexylcarbodiimide (DCC) predissolved in anhydrous CH_2Cl_2 was then added dropwise to the stirring mixture. After the addition, the reaction mixture was allowed to stir at 0 °C for 5 min and then warmed to room temperature overnight. Then the precipitated solids were removed by gravity filtration; the filtrate was washed with a dilute solution of sodium bicarbonate ($NaHCO_3$) and water and finally dried over Na_2SO_4. The solution was filtered and the solvent was removed under vacuum evaporation. The crude products were further purified by silica gel column chromatography using a mixture of 4:1 CH_2Cl_2/hexane as the eluent.

Synthesis of Methyl 4-(Pent-4-enyloxy)benzoate (G1ME). The reaction mixture of 4.90 g (32.86 mmol) of 5-bromopentene, 5.40 g (35.58 mmol) of methyl 4-hydroxybenzoate, 32.0 g of K_2CO_3, and 92 mg of 18-crown-6 in 400 mL of acetone afforded 6.0 g of oil product in 82.9% yield. ^{1}H NMR ($CDCl_3$): δ (ppm) 7.97 (2H, d, $J = 9.0$ Hz), 6.89 (2H, d, $J = 9.0$ Hz), 5.94 (1H, ddt,

J = 19.8, 10.5, 6.6 Hz), 5.13 (2H, ddt, J = 17.7, 17.1, 1.5 Hz), 4.00 (3H, t, J = 6.6 Hz), 3.87 (3H, s), 2.24 (2H, dd, J = 11.1, 5.1 Hz), 1.89 (2H, dt, J = 14.4, 6.6 Hz).

Synthesis of 4-(Pent-4-enyloxy)phenylmethanol (G1MOH). The reaction mixture of 3.80 g (17.25 mmol) of G1ME and 0.98 g (25.88 mmol) of LAH in 120 mL of THF afforded 3.13 g of oil product in 94.4% yield. ^{1}H NMR ($CDCl_3$): δ (ppm) 7.34 (2H, d, J = 8.1 Hz), 6.96 (2H, d, J = 8.4 Hz), 5.94 (1H, ddt, J = 17.1, 10.5, 6.6 Hz), 5.13 (2H, ddt, J = 17.7, 17.1, 1.5 Hz), 4.65 (2H, s), 4.05 (2H, t, J = 6.6 Hz), 2.33 (2H, dd, J = 11.1, 5.1 Hz), 2.24 (1H, s), 1.97 (2H, dt, J = 14.4, 6.6 Hz).

Synthesis of 4-(Pent-4-enyloxy)benzoic Acid (G1MCOOH). The reaction mixture of 1.00 g (4.54 mmol) of G1ME and 1.2 g of KOH in a mixed solvent of 15 mL of THF, 10 mL of EtOH, and 1.5 mL of H_2O afforded 0.86 g of oil product in 91.9% yield. ^{1}H NMR ($CDCl_3$): δ (ppm) 8.06 (2H, d, J = 9.0 Hz), 6.94 (2H, d, J = 9.0 Hz), 5.86 (1H, ddt, J = 17.1, 10.5, 6.6 Hz), 5.04 (2H, ddt, J = 17.7, 17.1, 1.5 Hz), 4.04 (t, 2H, J = 6.6 Hz), 2.26 (2H, dd, J = 11.1, 5.1 Hz), 1.92 (2H, dt, J = 14.4, 6.6 Hz).

Synthesis of 2-(2,5-Di(thiophen-2-yl)thiophen-3-yl)ethyl 4-(Pent-4-enyloxy)benzoate (G1M3T). The reaction mixture of 0.65 g (3.15 mmol) of G1MCOOH, 1.10 g (3.78 mmol) of 3TOH, 0.78 g (3.78 mmol) of DCC, and 0.0464 g (0.38 mmol) of DMAP in 15 mL of CH_2Cl_2 afforded 1.14 g of dark green oil product in 75.1% yield. ^{1}H NMR ($CDCl_3$): δ (ppm) 7.95 (2H, d, J = 8.7 Hz), 7.35−7.00 (7H, m), 6.89 (2H, d, J = 8.7 Hz), 5.85 (1H, ddt, J = 17.1, 10.5, 6.6 Hz), 5.04 (2H, ddt, J = 17.7, 17.1, 1.5 Hz), 4.53 (2H, t, J = 6.6 Hz), 4.02 (2H, t, J = 6.6 Hz), 3.21 (2H, t, J = 7.2 Hz), 2.25 (2H, dd, J = 11.1, 5.1 Hz), 1.90 (dt, 2H, J = 14.4, 6.6 Hz).

Synthesis of Methyl 3,5-Bis(4-(pent-4-enyloxy)benzyloxy)-benzoate (G2ME). The reaction mixture of 4.20 g (21.8 mmol) of G1MOH, 1.93 g (11.5 mmol) of methyl 3,5-dihydroxybenzoate, 5.72 g of PPh_3 (21.8 mmol), and 4.41 g (21.8 mmol) of DIAD in 15 mL of THF afforded 4.25 g of oil product in 75.4% yield. ^{1}H NMR ($CDCl_3$): δ (ppm) 7.40−6.47 (11H, m), 5.85 (2H, ddt, J = 17.1, 10.5, 6.6 Hz), 5.14−4.83 (8H, m), 4.10−3.87 (4H, m), 3.83 (3H, s), 2.24 (4H, dd, J = 11.1, 5.1 Hz), 1.90 (4H, dt, J = 14.4, 6.6 Hz).

Synthesis of 3,5-Bis(4-(pent-4-enyloxy)benzyloxy)benzoic Acid (G2MCOOH). The reaction mixture of 1.33 g (2.57 mmol) of G2ME and 0.8 g of KOH in a mixed solvent of 10 mL of THF, 8 mL of EtOH, and 0.8 mL of H_2O afforded 1.16 g of oil product in 90.0% yield. ^{1}H NMR ($CDCl_3$): δ (ppm) 7.42−6.48 (11H, m), 5.86 (2H, ddt, J = 17.1, 10.5, 6.6 Hz), 5.17−4.86 (8H, m), 4.12−3.88 (4H, m), 2.26 (4H, dd, J = 11.1, 5.1 Hz), 1.92 (4H, dt, J = 14.4, 6.6 Hz).

Synthesis of 2-(2,5-Di(thiophen-2-yl)thiophen-3-yl)ethyl 3,5-Bis-(4-(pent-4-enyloxy)benzyloxy)benzoate (G2M3T). The reaction mixture of 0.74 g (1.47 mmol) of G2MCOOH, 0.516 g (1.76 mmol) of 3TOH, 0.361 g (1.76 mmol) of DCC, and 0.0215 g (0.176 mmol) of DMAP in 10 mL of CH_2Cl_2 afforded 0.83 g of dark green oil product in 72.8% yield. ^{1}H NMR ($CDCl_3$): δ (ppm) 7.42−6.48 (18H, m), 5.86 (2H, ddt, J = 17.1, 10.5, 6.6 Hz), 5.17−4.86 (8H, m), 4.51 (2H, t, J = 6.6 Hz), 4.12−3.88 (4H, m), 3.18 (2H, t, J = 7.2 Hz), 2.25 (4H, dd, J = 11.1, 5.1 Hz), 1.91 (4H, dt, J = 14.4, 6.6 Hz).

Synthesis of Methyl 3,5-Bis(pent-4-enyloxy)benzoate (G1DE). The reaction mixture of 5.40 g (36.23 mmol) of 5-bromopentene, 3.35 g (19.93 mmol) of methyl 3,5-dihydroxybenzoate, 35.0 g of K_2CO_3, and 108 mg of 18-crown-6 in 400 mL of acetone afforded 4.68 g of oil product in 84.9% yield. ^{1}H NMR ($CDCl_3$): δ (ppm) 7.16 (2H, d, J = 2.4 Hz), 6.63 (2H, d, J = 2.4 Hz), 5.85 (2H, ddt, J = 17.1, 10.5, 6.6 Hz), 5.03 (4H, ddt, J = 17.7, 17.1, 1.5 Hz), 3.98 (4H, t, J = 6.6 Hz), 3.89 (3H, s), 2.23 (4H, dd, J = 11.1, 5.1 Hz), 1.88 (4H, dt, J = 14.4, 6.6 Hz).

Synthesis of (3,5-Bis(pent-4-enyloxy)phenyl)methanol (G1DOH). The reaction mixture of 6.23 g (24.47 mmol) of G1DE and 1.39 g (30.70 mmol) of LAH in 150 mL of THF afforded 6.27 g of oil product in 92.8% yield. ^{1}H NMR ($CDCl_3$): δ (ppm) 6.50 (2H, d, J = 2.1 Hz), 6.38 (2H, t, J = 2.4 Hz), 5.85 (2H, ddt, J = 17.1, 10.5, 6.6 Hz), 5.03 (4H, ddt, J = 17.7, 17.1, 1.5 Hz), 4.61 (2H, s), 3.95 (2H, t, J = 6.6 Hz), 2.23 (4H, dd, J = 11.1, 5.1 Hz), 1.87 (4H, dt, J = 14.4, 6.6 Hz), 1.78 (1H, s).

Synthesis of 3,5-Bis(pent-4-enyloxy)benzoic Acid (G1DCOOH). The reaction mixture of 2.25 g (7.39 mmol) of G1DE and 2.0 g of KOH in a mixed solvent of 15 mL of THF, 10 mL of EtOH, and 2.0 mL of H_2O afforded 1.96 g of oil product in 91.2% yield. ^{1}H NMR ($CDCl_3$): δ (ppm) 7.23 (2H, d, J = 2.4 Hz), 6.69 (2H, t, J = 2.4 Hz), 5.86 (2H, ddt, J = 17.1, 10.5, 6.6 Hz), 5.04 (4H, m), 4.00 (4H, t, J = 6.6 Hz), 2.25 (4H, dd, J = 11.1, 5.1 Hz), 1.90 (4H, dt, J = 14.4, 6.6 Hz).

Synthesis of 2-(2,5-Di(thiophen-2-yl)thiophen-3-yl)ethyl 3,5-Bis(pent-4-enyloxy)benzoate (G1D3T). The reaction mixture of 1.86 g (6.41 mmol) of G1DCOOH, 1.82 g (6.22 mmol) of 3TOH, 1.32 g (6.41 mmol) of DCC, and 0.0783 g (0.64 mmol) of DMAP in 25 mL of CH_2Cl_2 afforded 2.85 g of green or yellow oil product in 81.5% yield. ^{1}H NMR ($CDCl_3$): δ (ppm) 7.35−7.00 (9H, m), 6.63 (1H, t, J = 2.4 Hz), 5.85 (2H, ddt, J = 17.1, 10.5, 6.6 Hz), 5.03 (4H, m), 4.55 (2H, t, J = 6.9 Hz), 3.94 (4H, t, J = 6.6 Hz), 3.22 (2H, t, J = 6.6 Hz), 2.22 (4H, dd, J = 11.1, 5.1 Hz), 1.86 (4H, dt, J = 14.4, 6.6 Hz).

Synthesis of Methyl 3,5-bis(3,5-bis(pent-4-enyloxy)benzyloxy)-benzoate (G2DE). The reaction mixture of 5.26 g of G1DOH (19.0 mmol), 1.76 g (10.5 mmol) of methyl 3,5-dihydroxybenzoate, 4.98 g (19.0 mmol) of PPh_3, and 3.84 g (19.0 mmol) of DIAD in 15 mL of THF afforded 4.86 g of oil product in 78.9% yield. ^{1}H NMR ($CDCl_3$): δ (ppm) 7.29 (2H, d, J = 2.1 Hz), 6.79 (1H, t, J = 2.1 Hz), 6.56 (4H, d, J = 2.1 Hz), 6.41 (2H, t, J = 2.1 Hz), 5.85 (4H, ddt, J = 17.1, 10.5, 6.6 Hz), 5.05 (8H, m), 4.99 (4H, s), 3.96 (8H, t, J = 6.6 Hz), 3.91 (3H, s), 2.24 (8H, dd, J = 11.1, 5.1 Hz), 1.88 (8H, dt, J = 14.4, 6.6 Hz).

Synthesis of 3,5-Bis(3,5-bis(pent-4-enyloxy)benzyloxy)benzoic Acid (G2DCOOH). The reaction mixture of 2.11 g (3.08 mmol) of G2DE and 1.0 g of KOH in a mixed solvent of 15 mL of THF, 10 mL of EtOH, and 1.0 mL of H_2O afforded 1.84 g of oil product in 89.1% yield. ^{1}H NMR ($CDCl_3$): δ (ppm) 7.33 (2H, d, J = 2.4 Hz), 6.83 (2H, t, J = 2.4 Hz), 6.56 (4H, d, J = 2.1 Hz), 6.41 (2H, t, J = 2.1 Hz), 5.85 (4H, ddt, J = 17.1, 10.5, 6.6 Hz), 5.04 (8H, m), 5.00 (4H, s), 3.96 (8H, t, J = 6.6 Hz), 2.24 (8H, dd, J = 11.1, 5.1 Hz), 1.88 (8H, dt, J = 14.4, 6.6 Hz).

Synthesis of 2-(2,5-Di(thiophen-2-yl)thiophen-3-yl)ethyl 3,5-Bis-(3,5-bis(pent-4-enyloxy)benzyloxy)benzoate (G2D3T). The reaction mixture of 1.37 g (2.04 mmol) of G2DCOOH, 0.716 g (2.45 mmol) of 3TOH, 0.505 g (2.45 mmol) of DCC, and 0.0299 g (0.245 mmol) of DMAP in 15 mL of CH_2Cl_2 afforded 1.43 g of green or yellow solid product in 74.0% yield. ^{1}H NMR ($CDCl_3$): δ (ppm) 7.34−6.95 (9H, m), 6.78 (1H, t, J = 2.4 Hz), 6.54 (4H, d, J = 2.1 Hz), 6.41 (2H, t, J = 2.1 Hz), 5.85 (4H, ddt, J = 17.1, 10.5, 6.6 Hz), 5.04 (8H, m), 4.93 (4H, s), 4.56 (2H, t, J = 6.9 Hz), 3.95 (8H, t, J = 6.6 Hz), 3.23 (2H, t, J = 6.9 Hz), 2.24 (8H, dd, J = 11.1, 5.1 Hz), 1.87 (8H, dt, J = 14.4, 6.6 Hz).

Synthesis of Methyl 3,4,5-Tris(pent-4-enyloxy)benzoate (G1TE). The reaction mixture of 6.76 g (45.36 mmol) of 5-bromopentene, 2.68 g (14.56 mmol) of methyl 3,4,5-trihydroxybenzoate, 40.0 g of K_2CO_3, and 125 mg of 18-crown-6 in 400 mL of acetone afforded 4.87 g of oil product in 86.0% yield. ^{1}H NMR ($CDCl_3$): δ (ppm) 7.27 (2H, s), 5.94−5.77 (3H, m), 5.02 (6H, m), 4.04 (6H, dt, J = 6.6, 6.0 Hz), 3.89 (3H, s), 2.34−2.21 (6H, m), 2.34−2.21 (6H, m).

Synthesis of (3,4,5-Tris(pent-4-enyloxy)phenyl)methanol (G1TOH). The reaction mixture of 5.34 g (13.75 mmol) of G1TE and 0.782 g (20.62 mmol) of LAH in 100 mL of THF afforded 4.62 g of oil product in 93.2% yield. ^{1}H NMR ($CDCl_3$): δ (ppm) 6.50 (2H, s), 5.94−5.77 (3H, m), 5.01 (6H, m), 4.50 (2H, s), 3.95 (6H, dt, J = 6.6, 6.0 Hz), 2.62 (1H, s), 2.32−2.19 (6H, m), 1.94−1.78 (6H, m).

Synthesis of 3,4,5-Tris(pent-4-enyloxy)benzoic Acid (G1TCOOH). The reaction mixture of 2.11 g (3.08 mmol) of G1TE and 1.0 g of

KOH in a mixed solvent of 15 mL of THF, 10 mL of EtOH, and 1.0 mL of H_2O afforded 1.84 g of oil product in 89.1% yield. ^{1}H NMR ($CDCl_3$): 8.98 (1H, b), 7.33 (2H, s), 5.94−5.78 (3H, m), 5.03 (6H, m), 4.06 (6H, dt, J = 10.8, 6.3 Hz), 2.32−2.21 (6H, m), 1.94−1.80 (6H, m).

Synthesis of 2-(2,5-Di(thiophen-2-yl)thiophen-3-yl)ethyl 3,4,5-Tris(pent-4-enyloxy)benzoate (G1T3T). The reaction mixture of 1.37 g (2.04 mmol) of G1TCOOH, 0.716 g (2.45 mmol) of 3TOH, 0.505 g (2.45 mmol) of DCC, and 0.0299 g (0.245 mmol) of DMAP in 15 mL of CH_2Cl_2 afforded 1.43 g of green or yellow solid product in 74.0% yield. ^{1}H NMR ($CDCl_3$): δ (ppm) 7.36−7.00 (9H, m), 5.98−5.80 (3H, m), 5.05 (6H, m), 4.59 (2H, t, J = 6.9 Hz), 4.08 (2H, t, J = 6.3 Hz), 3.98 (4H, t, J = 6.3 Hz), 3.25 (2H, t, J = 6.6 Hz), 2.37−2.21 (6H, m), 1.97−1.83 (6H, m).

Synthesis of Methyl 3,5-Bis(3,4,5-tris(pent-4-enyloxy)benzyloxy)-benzoate (G2TE). The reaction mixture of 5.31 g (14.73 mmol) of G1TOH, 1.13 g (6.69 mmol) of methyl 3,5-dihydroxybenzoate, 3.86 g (14.73 mmol) of PPh_3 and 2.98 g (14.73 mmol) of DIAD in 12 mL of THF afforded 3.94 g of oil product in 69.0% yield. ^{1}H NMR ($CDCl_3$): δ (ppm) 7.30 (1H, d, J = 2.4 Hz), 6.82−6.36 (6H, m), 5.95−5.76 (6H, m), 5.10−4.96 (12H, m), 4.96 (4H, s), 3.99 (12H, t, J = 6.3 Hz), 3.91 (3H, s), 2.34−2.18 (12H, m), 1.97−1.79 (12H, m).

Synthesis of 3,5-Bis(3,4,5-tris(pent-4-enyloxy)benzyloxy)benzoic Acid (G2TCOOH). The reaction mixture of 2.44 g (2.86 mmol) of G2TE and 1.0 g of KOH in a mixed solvent of 15 mL of THF, 10 mL of EtOH, and 1.0 mL of H_2O afforded 2.03 g of oil product in 83.2% yield. ^{1}H NMR ($CDCl_3$): δ (ppm) 7.28 (1H, d, J = 2.4 Hz), 6.80−6.33 (6H, m), 5.94−5.75 (6H, m), 5.11−4.96 (12H, m), 4.96 (4H, s), 3.99 (12H, t, J = 6.3 Hz), 2.34−2.18 (12H, m), 1.97−1.79 (12H, m).

Synthesis of 2-(2,5-Di(thiophen-2-yl)thiophen-3-yl)ethyl 3,5-Bis-(3,4,5-tris(pent-4- enyloxy)benzyloxy)benzoate (G2T3T). The reaction mixture of 1.18 g (1.41 mmol) of G2TCOOH, 0.494 g (1.69 mmol) of 3TOH, 0.349 g (1.69 mmol) of DCC, and 0.0208 g (0.17 mmol) of DMAP in 10 mL of CH_2Cl_2 afforded 1.12 g of dark green oil product in 71.3% yield. ^{1}H NMR ($CDCl_3$): δ (ppm) 7.33−6.93 (7H, m), 6.81−6.36 (6H, m), 5.96−5.77 (6H, m), 5.11−4.95 (12H, m), 4.89 (4H, s), 4.57 (2H, t, J = 7.2 Hz), 3.99 (12H, t, J = 6.3 Hz), 3.23 (2H, t, J = 6.6 Hz), 2.35−2.20 (12H, m), 1.97−1.82 (12H, m).

2.4. Surface-Initiated Ring-Opening Metathesis Polymerization (SI-ROMP) of Norbornene on the Electropolymerized Films. Norbornene was chosen as the monomer for demonstrating SI-ROMP on the electropolymerized films because it is commercially available and is facile in the ring-opening process. All the SI-ROMP was conducted in a glovebox under a N_2 atmosphere. The electropolymerized films were first immersed into a 0.35 M of the first generation Grubbs catalyst solution in CH_2Cl_2 for 30 min to activate the surfaces. Then the films were washed consecutively three times with CH_2Cl_2 to completely remove any unbound catalyst. After washing, the catalyst-activated slides were immediately dipped into a 0.2 M norbornene monomer solution in CH_2Cl_2 up to 60 min. In the kinetics studies, a slide at a certain time interval was taken out from the monomer solution followed by copious washing with CH_2Cl_2. A total of six slides for each kinetics study were used to plot the polymer growth curve.

2.5. Ellipsometric Measurement of the Film Thickness before and after SI-ROMP. After electropolymerization of the dendron and after the SI-ROMP, the samples were dried completely and the film thickness was measured by ellipsometry (HeNe laser, 632 nm). The incident angle was fixed at 70° on the gold electrode samples. The thickness value was averaged by taking six different spots on the polymer films. The refractive indices of the electropolymerized films and the resulting polymer brush films were assumed to be 1.45 and 1.50, respectively.

3. Results and Discussion

3.1. Synthesis of the Electropolymerizable Peripheral Olefin Dendrons. Peripheral olefin dendrons as building blocks for dendrimers which can be cross-linked at the peripheries via ring-closing metathesis reaction has been reported by Zimmerman et al.[20−23] These dendrimers have found interesting applications especially in host−guest chemistry. Shon and Choi have recently synthesized gold nanoparticles capped with peripheral olefin dendron thiols prepared by a convergent approach.[24] In our present work, the synthesis of an electropolymerizable dendron molecule was achieved by Steglich esterification of 2,2′:5′,2″-terthiophene ethanol (3TOH) with the Frechet-type peripheral olefin dendrons at the carboxylic acid foci in the presence of DCC and DMAP. In this manner, the electrochemically active terthiophene moiety was attached at the focal point of the dendron. The commercially available methyl benzoate with mono-, di-, and trihydroxy on the phenyl groups offers a facile pathway to vary the number of terminal olefins, as shown in Schemes 2, 3, and 4, respectively. Mitsunobu coupling reaction was applied to bring the first-generation dendrons onto the 3- and 5-positions of the dihydroxymethyl benzoate, giving the second-generation dendrons. This coupling reactions were either carried out by conventional synthesis methods involving reflux or by the sonication-assisted approach reported in our group.[18]

3.2. Electropolymerization of the Terminal Olefin Dendrons. 2,2′:5′,2″-Terthiophene containing monomers and polymers have shown very good electroactivity in device applications, nanopatterning and electrochromic devices, etc.[19,25−27] The electrochemical oxidation of the terthiophene unit toward polymer synthesis is more facile compared to thiophene and carbazole in that it has a lower oxidation potential.[19] Herein we studied their electropolymerizability as dendronized monomers.

3.2.1. Electropolymerization of the First-Generation Terminal Olefin Dendrons. Electropolymerization was done first with the first-generation dendrons on bare gold and ITO. Although typical CV curves for electropolymerization of the terthiophene molecules were obtained, the polymer films were partially washed away by THF or CH_2Cl_2. This can be attributed to the poor adhesion of the polythiophene films which is only physically adsorbed on the electrode surfaces. It is not unreasonable considering that dendritic side chains enhances polythiophene solubility compared to alkyl side chains. In order to improve polymer film adhesion, a 11-(9*H*-carbazol-9-yl)undecane-1-thiol (CbzC11SH) or 9-(11-(trimethoxysilyl)undecyl)-9*H*-carbazole or (CbzC11-Silane) was used to modify the gold or ITO electrode surfaces. The synthesis of the thiol or silane molecule was reported in our earlier publications.[16,17] 5 mM of the thiol or silane was used to prepare a monolayer film. More specifically, the carbazole-terminated alkylsilane was dissolved in toluene, and the ITO electrodes were then immersed in this solution at 60 °C for 12 h. The carbazole-terminated alkylthiol solution in THF was used to functionalize the gold electrodes for 2 h. The electrodes were examined by AFM, before and after the procedure. As shown in Figure S1 (Supporting Information), the silane-functionalized ITO surfaces exhibited a more "fuzzy" morphology with aggregates compared to the clear boundaries on bare ITO surface. Ellipsometric measurements on the CbzC11SH-modified gold electrode gave a film thickness ~1.1 nm, indicating monolayer surface coverage. During the electropolymerization process, the carbazole moieties in the SAMs should be copolymerized (electrografted) with the terthiophene units, leading to covalent linkages or chemical adhesion between the SAM-modified electrode surface and the polythiophene films. As expected, the electropolymerized films exhibited much better resistance to solvent washing. Even after sonication in good solvents like THF and CH_2Cl_2, the film thickness was maintained.

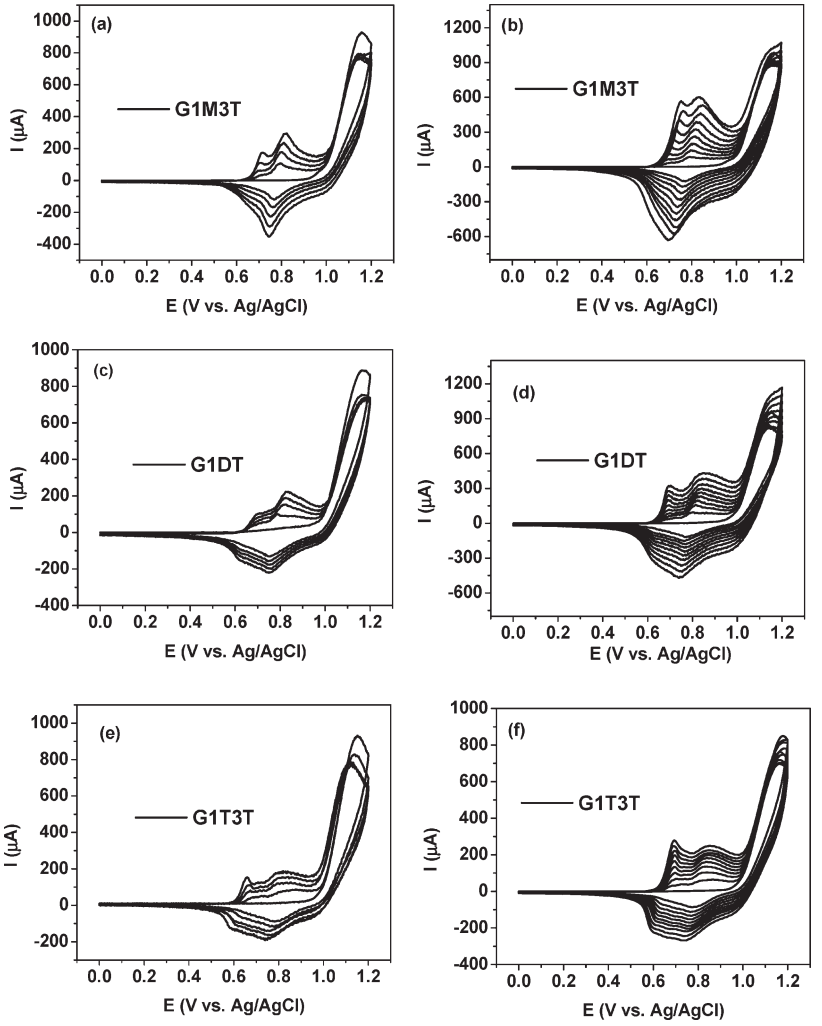

Figure 2. CV of the dendrons after 5 CV cycles (G1M3T, a; G1D3T, c; and G1T3T, e) and 10 CV cycles (G1M3T, b; G1D3T, d; and G1T3T, f). The CV measurements were carried out in 5 mM of each monomer in 0.1 M of $TBAPF_6$ solution in acetonitrile. Potential scan window: 0−1.2 V; scan rate: 50 mV/s; reference electrode: Ag/AgCl; counter electrode: Pt wire; working electrode: ITO.

The CV experiments were carried out in different solvent systems including THF, CH_2Cl_2, and acetonitrile (ACN). Electropolymerization in ACN gave the highest film thickness and the best quality film morphology in terms of surface roughness and homogeneity. To determine the effect of electropolymerized film thickness on polymer brush growth, we applied 5 and 10 CV cycles and compared brush thickness and polymer brush growth kinetics. The CV traces for 5 cycles are presented in Figure 2. In the first cycles, the monomer oxidation peak position for all three dendrons was found at almost the same position at 1.15 V. Upon scanning in a reverse direction, the reduction peak around 0.75 V showed a significantly lower current. With the succeeding scans, two new oxidation waves appeared between 0.6 and 1.0 V, corresponding to the oxidation of the newly formed polythiophene from the first scan. However, they were not observed from CV results of a previous report on polynorbornene bearing terthiophene in the side chains using ACN as the solvent.[28] Also, only a single polymer oxidation peak was observed from the CV curves using THF and CH_2Cl_2 as the solvent. These differences may be related to polythiophene oxidation with formation of two electronic transitions: polarons and bipolaron species in a stepwise manner. The polymerization oxidation process most likely occurs at the same time scale with the doping and dedoping of the already deposited polymer. Previously, in situ electron spin resonance (ESR) and optical measurements on polythiophenes have shown that spinless species (bipolarons) are generated at the maximum oxidation level of each step and spin-bearing species (polarons) produced at an intermediate oxidation in the first process only.[29] Usually, low-temperature CV measurements are done to observe the two peaks in which ion transport is very slow. In this case, the use of the ACN solvent and the dendronized monomer perhaps gives a better resolution of this two-step doping process by a better control of thickness and a more restricted internal morphology in terms of ion transport. Further investigation into the redox properties and polaronic structures of the polymers, e.g., by spectroelectrochemistry or low-temperature measurements, may help understand this phenomenon better.

The cathodic waves from 1.0 to 0.4 V correspond to the reduction process from the oxidized and conductive polythiophenes to their neutral state (dedoping). Two partially separated reduction peaks were similarly observed, with each correlating with the corresponding oxidation peaks. Repeated cycles showed an even growth interval in both oxidation and reduction currents, which is in agreement with the cyclic deposition of the electroactive polymer films. This suggests that the olefins in these dendrons are not involved in the electropolymerization.[30,31] Moreover, vinyl groups are known to polymerize only under negative potential cathodic electropolymerization conditions through radical anion mechanisms.[8−10,14]

Table 1. Anodic and Cathodic Peak Potentials and Currents on the Final Scans from the CV of the First-Generation Dendrons[a]

films	E^1_{pa}	E^2_{pa}	i^1_{pa}	i^2_{pa}	E^1_{pc}	E^2_{pc}	i^1_{pc}	i^2_{pc}
G1M3T_5	0.71	0.82	171.3	290.5		0.74		−351.0
G1M3T_10	0.75	0.83	565.0	600.5		0.70		−623.7
G1D3T_5	0.70	0.83	104.0	221.9	0.62	0.75	−149.2	−217.7
G1D3T_10	0.71	0.85	318.4	433.1	0.63	0.74	−321.4	−464.7
G1T3T_5	0.66	0.83	152.1	184.2	0.61	0.74	−134.8	−185.8
G1T3T_10	0.69	0.86	275.8	249.5	0.60	0.73	−224.2	−268.1

[a] The units for anodic and cathodic peak potentials are V, and the units for anodic and cathodic peak currents are μA. Because of the serious overlap of the reduction waves for G1M3T, only the peak at the higher position was included in this table. The onset for all the CV curves is at 0.57 V. G1M3T_5: electrografted polythiophene films after 5 CV cycles from G1M3T. 1 donates the higher oxidation/reduction peak, and 2 donates the lower oxidation/reduction peak. E_{pa}: anodic peak potential; i_{pa}: anodic peak current; E_{pc}: cathodic peak potential; i_{pc}: cathodic peak current.

In all cases, the oxidation peaks moved to higher potentials and the reduction peaks shifted toward lower potentials. This gradually broadened peak separation is a typical feature for semiconducting polymer electrodeposition.[29] As more polymers are electrochemically grafted onto the electrodes, the electron transfer kinetics in turn becomes more heterogeneous. It should be noted that even though some polythiophenes were copolymerized with the SAM carbazole groups on the first cycle, a certain amount of polymers would still redissolve into the supporting electrolyte solution with subsequent cycles.[16−18] The dissolved polymers doped with the anions were visibly seen from the much darker orange color of the electrolyte solution compared to the light green or yellow starting monomer−electrolyte solution. As good solvents like THF and CH_2Cl_2 were used, the electrolyte solutions after electropolymerization were even deeper orange in color, giving further evidence of more dissolved polymer species. The CV experiments on the CbzC11SH-covered gold electrodes showed similar results. Note that all thicknesses after electropolyermization and SI-ROMP procedure were measured by ellipsometry on these gold electrodes.

Table 1 summarizes the CV results in terms of oxidative and reductive peak potentials and currents from the final scan. There is no distinct difference in both the onset and the peaks of the anodic (oxidative) and cathodic (reductive) waves for all the three dendrons. Only slightly lower anodic peaks (~50 mV) were observed with G1T3T. All these observations reveal that the olefin dendron side chains have negligible effects on the electrochemical reactivity of the terthiophene moiety and the polythiophene film formation.[8−10] Interestingly, both polymer oxidation and reduction peak currents decreased with increasing number of olefin peripheral groups on changing from G1M3T to G1D3T to G1T3T. This is mainly attributed to a decreased tendency to deposit more material per cycle on the electrode (perhaps a decrease in molecular weight of the polythiophene as well). More branching can hinder terthiophene reactivity and highly branched side chains on the formed polymer increases polymer solubility, thereby reducing its adhesion on the surface. The lowest molecular weights and the smallest polymer aggregates would then be expected from G1T3T. In contrast, electropolymeriation of G1M3T would tend to give longer polymer chains or bigger aggregates on the electrode surfaces (as shown later by AFM).

Moreover, the polymer oxidation and reduction waves were reversible as evidenced by the comparable peak currents. This means that the electron transfer rate is faster than the scan rate (50 mV/s) and that all oxidized and reduced polythiophene species deposited should be stable without any significant side reactions.

Table 2. Anodic and Cathodic Peak Potentials and Currents on the Final Scans from the CV of the Second-Generation Dendrons[a]

films	E_{pa}	i_{pa}	E_{pc}	i_{pc}
G2M3T_5	0.95	22.4	0.82	−53.9
G2M3T_10	0.93	59.9	0.79	−86.1
G2D3T_5	0.96	28.5	0.83	−33.8
G2D3T_10	0.85	91.1	0.67	−120.4
G2T3T_5	0.91	24.9	0.80	−50.8
G2T3T_10	0.98	26.9	0.87	−39.3

[a] G2M3T_5: electrografted polythiophene films after 5 CV cycles from G2M3T.

Table 3. Film Thicknesses Measured by Ellipsometry before and after 1 h SI-ROMP of Norbornene[a]

E-films	thickness (nm)	PNb films	thickness (nm)
E-G1M3T-5	27.2 ± 3.3	PNb-G1M3T-5	11.2 ± 2.2
E-G1D3T-5	22.5 ± 2.5	PNb-G1D3T-5	14.6 ± 2.7
E-G1T3T-5	18.7 ± 0.9	PNb-G1T3T-5	18.4 ± 3.1
E-G1M3T-10	41.3 ± 5.5	PNb-G1M3T-10	10.8 ± 2.4
E-G1D3T-10	35.7 ± 4.1	PNb-G1D3T-10	13.9 ± 3.0
E-G1T3T-10	30.5 ± 2.6	PNb-G1T3T-10	17.2 ± 3.3
E-G2M3T-5	5.2 ± 1.3	PNb-G2M3T-5	13.8 ± 0.9
E-G2D3T-5	4.7 ± 1.5	PNb-G2D3T-5	19.2 ± 1.1
E-G2T3T-5	16.3 ± 4.9	PNb-G2T3T-5	21.6 ± 2.9
E-G2M3T-10	7.7 ± 2.2	PNb-G2M3T-10	14.0 ± 1.0
E-G2D3T-10	22.7 ± 3.2	PNb-G2D3T-10	19.5 ± 1.3
E-G2T3T-10	18.5 ± 7.6	PNb-G2T3T-10	21.8 ± 6.5

[a] E-G1M3T-5 represents the electropolymerized film from G1M3T after 5 CV cycles under the listed conditions. PNb-G1M3T-5 represents the polynorbornene brush film on top of the electropolymerized films from G1M3T after 5 CV cycles.

3.2.2. Electropolymerization of the Second-Generation Peripheral Olefin Dendrons. Because of the limited solubility of the second-generation dendrons in ACN, THF was used as solvent. Except for the solvent used, all other conditions were the same as those in the electropolymerization of the first-generation dendrons. As shown in Figure S4 (Supporting Information), the CV traces appeared remarkably different from those of the first-generation dendrons in ACN. During the first scan, the monomer oxidation peaks were not well-defined. Nonetheless, in the retro scans, the CV waves in the range from 0.70 to 0.83 V corresponding to the polymer reductions are well behaved. In the following scans, the polymer oxidation and reduction were both significantly suppressed, similar to the first-generation dendrons using THF as solvent. As seen in Table 2, all the currents were about 1 order of magnitude lower than those obtained from Figure 2. In addition, the anodic and cathodic peak potentials were relatively higher. All these results strongly indicate that electropolymerization of these dendrons was not as favorable even in good solvents compared to the first generation. Thus, thinner films were obtained in this series of CV experiments (as measured by ellipsometry, shown in Table 3). Regardless of these observations, the films were still found to be stable against CH_2Cl_2 washing and even sonication or extraction, which is crucial for the SI-ROMP.

3.3. SI-ROMP of Norbornene on the Electropolymerized Films. Prior to SI-ROMP, the electropolymerized films were initially immersed in the first-generation Grubbs catalyst solutions for 30 min, leading to the Ru-activated surfaces. Any unbound ruthenium complexes were extensively washed by CH_2Cl_2 at least three times. Then the surface-activated sample was immediately dipped into a 0.2 M norbornene solution in CH_2Cl_2. After a specific period of time, a slide was taken out and washed with CH_2Cl_2. The polymerization was allowed to proceed up to 60 min at room temperature. The polynorbornene brush films were then investigated by AFM,

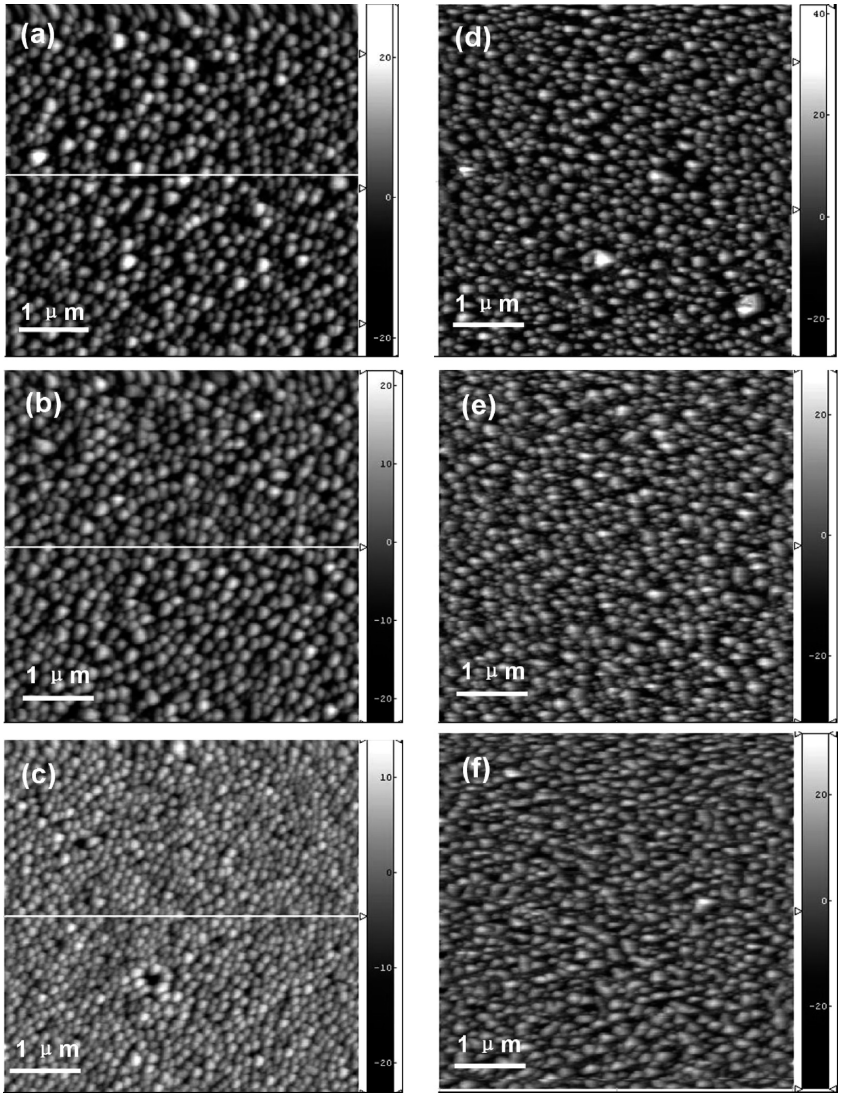

Figure 3. 2D tapping-mode AFM images of the electropolymerized films from the first-generation dendrons after 5 CV cycles (G1M3T, a; G1D3T, b; and G1T3T, c) and the polynorbornene (PNB) brush films grown on their corresponding electropolymerized films after 60 min (PNb-G1M3T-5, d; PNb-G1D3T-5, e; and PNb-G1T3T-5, f).

ellipsometry, and XPS to confirm the film surface morphology, thickness, and the atomic composition (elemental analysis).

3.3.1. AFM Study of the Electropolymerized Films and Polynorbornene Brush Films. The film morphology after electropolymerization of the dendrons before ROMP and after growth of polynorbornene brushes was examined by AFM. Figure 3 shows tapping-mode AFM images after electrografting of the first-generation dendrons with 5 CV cycles and after 1 h of SI-ROMP on their corresponding electropolymerized films. It can be seen that the polythiophene films highly covered the CbzC11-silane-modified ITO electrodes surface as compared with Figure S1b (Supporting Information). Similar surface morphology was also observed from the electropolymerized films with first-generation dendrons at 10 CV cycles, as presented in Figure S2 (Supporting Information). The AFM images (d, e, and f in Figure 3 and Figure S2) after SI-ROMP of norbornene on all electropolymerized films showed different morphologies based on the globule size shown in Table S1, which includes both the size of the globular features and the surface roughness from all the AFM images in Figure 3 and Figure S2. Although it is difficult to perform any quantitative analysis of the polymer brush density based on the AFM images alone, they are quite useful to allow us to confirm the successful growth of polymer brush and further compare the morphological changes before and after SI-ROMP. After 5 or 10 CV cycles, the size of those globular aggregates decreases from the electropolymerized films with G1M3T to G1T3T, in accordance with the discussions in the electropolymerization section.

The size of the globular and conical features from the polynorbornene films increases with dendron generation. More isolated islands are observed on the polymer brush film from the electropolymerized films with G1M3T. However, on the brush film from the electropolymerized films with G1T3T, the features become more interconnected. This also supports the fact that polymer brush growth can be controlled by changing the number of terminal olefin on the polythiophene side chains. Furthermore, the size of the aggregates before and after SI-ROMP, along with the surface roughness, is similar to both 5 and 10 CV cycles (Figure S2, Supporting Information). Therefore, once the electropolymerized films are fully covered by the dendrons, statistically the number of free olefins available from the polymer brush growth will only depend on the structure of the dendrons.

The surface morphology of the electropolymerized films from the second-generation dendrons in THF gave a much

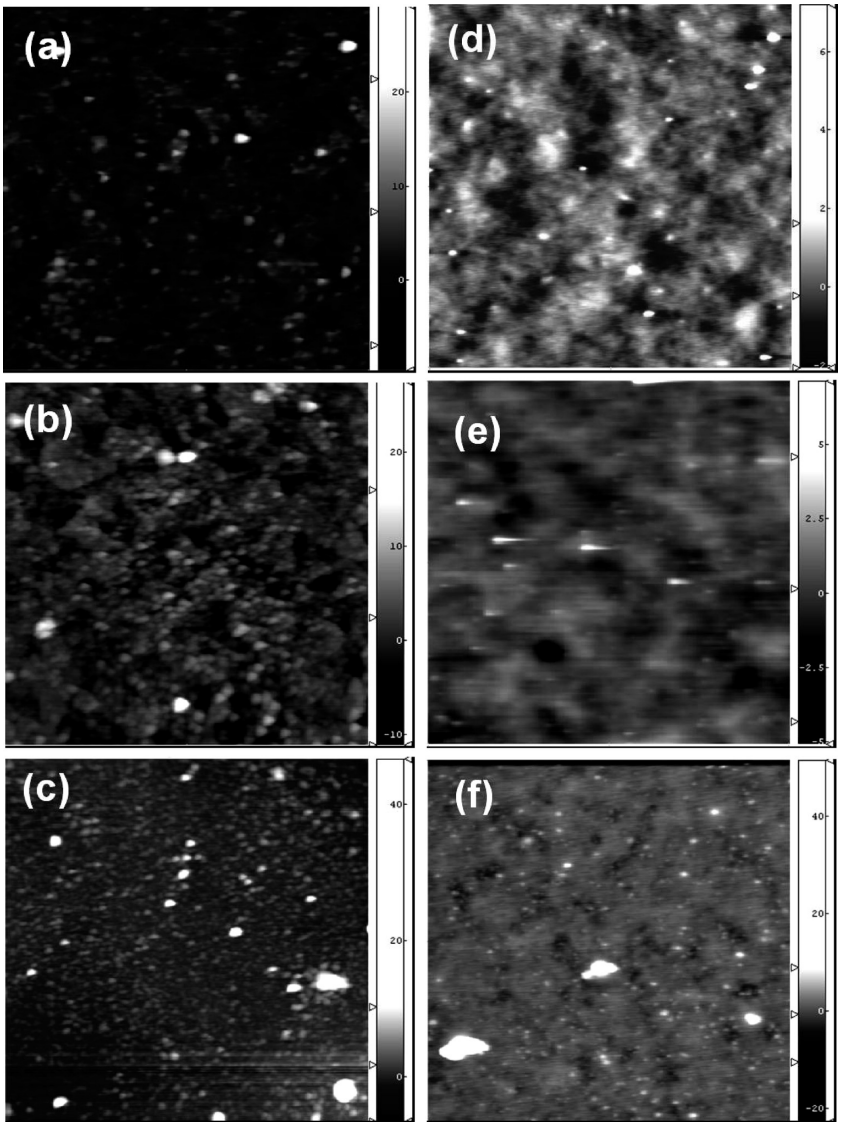

Figure 4. 2D tapping-mode AFM images of the electropolymerized films from the second-generation dendrons after 5 CV cycles (G2M3T, a; G2D3T, b; and G2T3T, c) and the polynorbornene brush films grown on their corresponding electropolymerized films (d, e, and f) after 60 min. All the images are $5 \times 5\ \mu m^2$.

different appearance, presumably due to solvent effects. In contrast to the densely packed globular features of polythiophene aggregates, the aggregates on the electropolymerized films in Figure 4 and Figure S3 are more isolated. The background of the ITO sharp domain edges is still visible. After SI-ROMP, the smoothness of polynorbornene films significantly improves, except for a few aggregates on the electropolymerized G2T3T films for both 5 and 10 CV cycles. The morphology of the polynorborne brush films here are actually very similar to those grown from surface-initiated films using SAMs.[4,32] In addition, there are some large pinholes or defects from the polymer brushes in all cases. The pinholes can have some unwanted effects for practical applications of the brush films, like electrical shorting in FET device fabrication, but they can usually be removed by thermal annealing.[3b]

3.3.2. Film Thicknesses of the Electropolymerized Films and the Polynorbornene Brush Films. To evaluate the effect of peripheral olefin number and the dendron generation on polymer brush growth, we measured the polymer brush thicknesses by ellipsometry. Table 3 summarizes the thickness values of the electropolymerized films and their corresponding polymer brush films on gold substrates. From G1M3T to G1T3T, in the case of both 5 and 10 CV cycles, an increase in polynorbornene brush thickness was observed. This is in contrast to a decrease in the electropolymerized film thickness during electrodeposition. This clearly demonstrates that the number of active olefins for ROMP on the electropolymerized films is statistically determined by the number of olefinic substituents present, which, in turn, controls polymer brush thickness as well as grafting density. Moreover, the thickness of the corresponding polynorbornene brush films increases disproportionally. By immersing the electropolymerized films from G1T3T into a 0.6 M of the Grubbs catalyst solution, no distinct thickness difference was obtained. This excludes the possibility that only a certain percentage of the free olefin functionalities are activated in the 0.35 M catalyst solution. One possible reason is that free olefins in the electropolymerized films from G1T3T are located in closer proximity. Therefore, there is a higher probability for cross-metathesis upon catalyst activation, although the vinyl-terminated functional groups are generally less susceptible with this catalyst. This can essentially decrease the density of the active sites for ROMP. To achieve a maximum polymer brush grafting density and the highest film thickness, in some

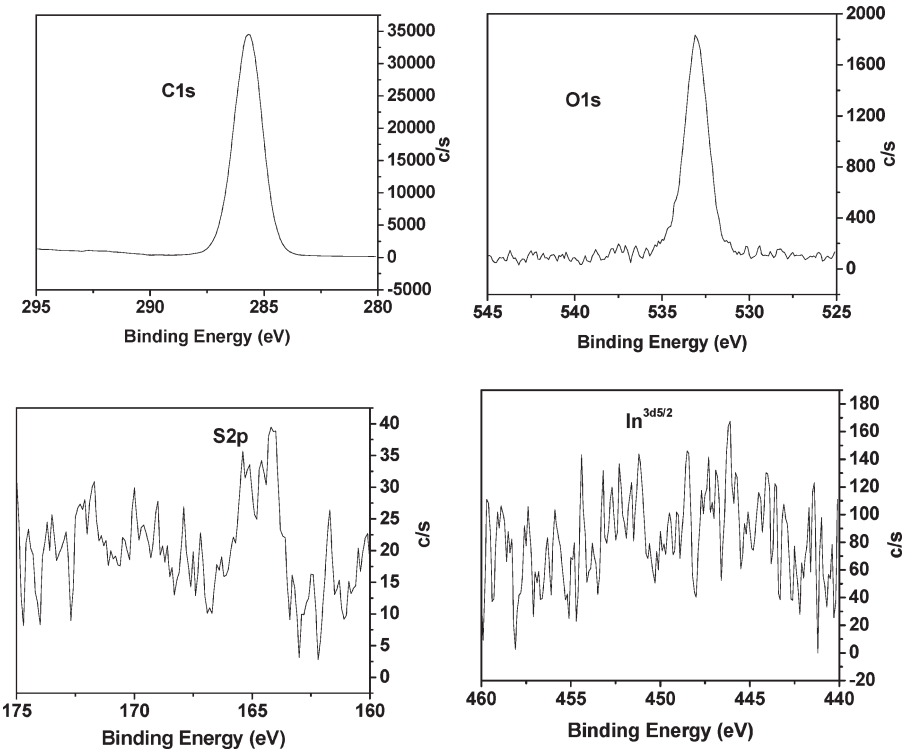

Figure 5. High-resolution XPS spectra of the C^{1s}, O^{1s}, S^{2p}, and $In^{3d_{5/2}}$ peaks on the polynorbornene-covered brush film grown from 5 CV cycle electropolymerized G2T3T (PNb-G2T3T-5).

cases, inert molecules were intentionally mixed into the surface initiator matrix to dilute the density of the active sites.[33] Another possible reason for this disproportionate thickness increase lies in the conformation of the side chains on the electrodeposited polythiophenes. This may be improved by thermal annealing.

No trend is found from the thickness of the electropolymerized films with the second-generation dendrons. Most of the thicknesses, in this series, are less than those of the first-generation dendrons electropolymerized in ACN. Nonetheless, polynorbornene brush thickness still increased from G2M3T to G2T3T, indicating the density of the free olefins still plays a key role in polymer brush growth even with thinner electrodeposited materials. By comparing G1D3T and G2M3T which both have two terminal olefin functional groups in each molecule, the brush film thickness were found identical, meaning the slightly larger G2M3T does not obviously change the statistical distribution of the effective olefinic sites. Again, a disproportionate relation between the electropolymerized film thickness and the number of peripheral olefins from the dendrons exists. Finally, the polynorbornene brush film thicknesses, in our study, are relatively lower than those grown from SAMs-activated surfaces with similar monomer concentration. This is perhaps due to a lower density of transition-metal-activated sites for ROMP.[34] Polymer brush synthesis on top of layer-by-layer (LBL) films containing initiators has been developed by the Armes group and our group very recently.[35−37] Polyelectrolyte macroinitiators were synthesized and then built into a multilayer architecture, leading to an amplified polymer brush growth by increasing porosity of the LBL films. On the other hand, using other chemically adsorbed macroinitiators on solid substrates provides another pathway to grow polymer brushes.[38] As a comparison, varying the number of peripheral olefins in our present work offers another useful method for polymer brush synthesis to control the growth of polymer brush.

Table 4. Relative Density of XPS Signals on the Polynorbornene Films Grown from the Electropolymerized Films with the Second-Generation Dendrons after 5 CV Cycles

films	C^{1s}	O^{1s}	S^{2p}	$In^{3d_{5/2}}$
PNb-G2M3T-5	95.82	3.01	0.07	1.10
PNb-G2D3T-5	97.30	2.15	0.08	0.47
PNb-G2T3T-5	97.39	2.57	0.04	0.00

3.3.3. XPS Analysis of the Electropolymerized Films and the Polynorbornene Brush Films. XPS analysis was performed at a takeoff angle of 45° for elemental analysis and surface content ratio. In the XPS study, we picked the brush films grown after 60 min from the electropolymerized films (5 CV cycles) with G2M3T, G2D3T, and G2T3T. High-resolution scans of the carbon (C), oxygen (O), sulfur (S), and indium (In) regions were obtained and then fitted with Gaussian equations for peak area analysis. Figure 5 shows a typical XPS spectra showing the 4 atom peaks in the film PNb-G2T3T-5. XPS data provide the qualitative and semiquantitative evidence of the presence of C^{1s} with a binding energy of 286 eV, O^{1s} with a binding energy of 533 eV, S^{2p} with a binding energy of 164 eV, and $In^{3d_{5/2}}$ with a binding energy of 445 eV. Table 4 shows the relative concentration of the C^{1s}, O^{1s}, S^{2p}, and $In^{3d_{5/2}}$ peaks on these films.

Evidently, the $In^{3d_{5/2}}$ peak is not present in the film PNb-G2T3T-5 which indicates the more highly dense and thicker brush, as supported by AFM and ellipsometry. As a comparison, the more porous and thinner film from PNb-G2M3T-5 shows the highest concentration of $In^{3d_{5/2}}$. Furthermore, the film PNb-G2T3T-5 provides the highest intensity of C^{1s} and the lowest intensity of S^{2p}. Additionally, the relative concentration of O^{1s} in the film PNb-G2T3T-5 is higher than that in the film PNb-G2D3T-5. It is not surprising that the theoretical percentage of oxygen atom in the dendron G2T3T is higher than that in G2D3T.

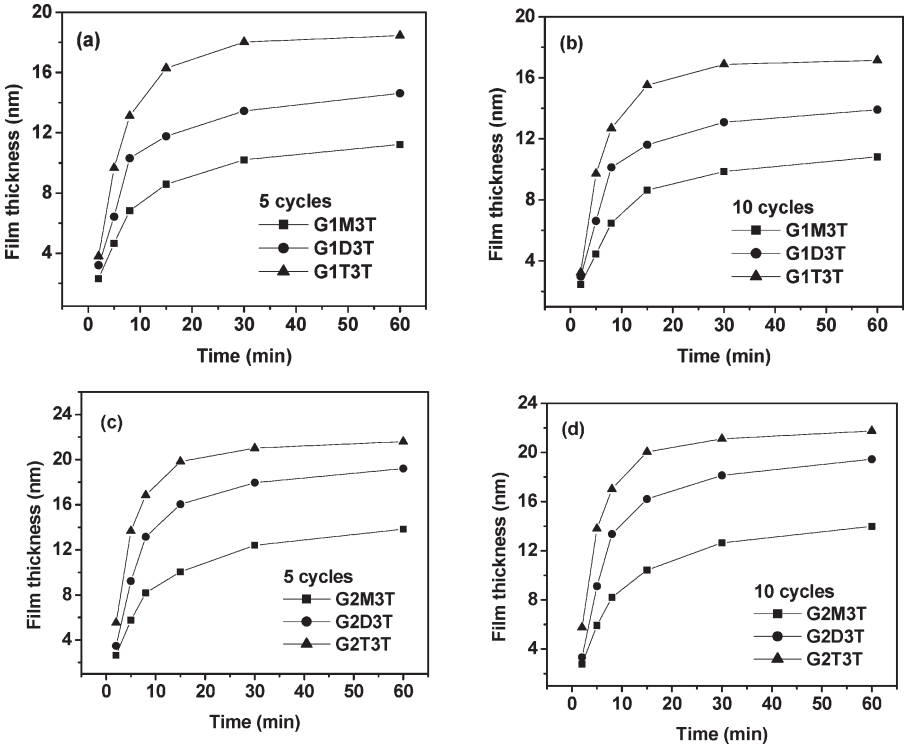

Figure 6. Ellipsometric film thicknesses of the polynorbornene brushes grown on the different electropolymerized films from the dendrons after 5 and 10 CV cycles.

3.3.4. Growth Kinetics of the Polynorbornene Brush Films. It is very important to understand polymer brush growth kinetics because it not only allows a better understanding of the basic fundamentals in film growth but also helps in the synthesis of polymer films with the desired thickness or grafting density. Recently, Jennings et al. have studied the kinetics of polynorbornene brush growth on the ROMP-active monolayer films based on some assumptions.[4] It was found that with increasing pendant alkyl chain length on norbornene monomer the growth kinetics of the polymer brush films drastically decreased by 2 orders of magnitude. Unfortunately, in our case, the growth kinetics in terms of initiation, propagation, and termination rate constants cannot be quantitatively analyzed, given that the density of the active olefins varies with a few parameters and hard to quantify. Thus, we attempted to qualitatively investigate the kinetics of the polynorbornene brushes grown on the electropolymerized films ex situ. As depicted in Figure 6, the polymers grow very rapidly in the first 20 min and then start to reach saturation slowly in the next 40 min. This is similar to previous reports on the measurements of polynorbornene (or their derivatives) growth kinetics.[3a,4] Therefore, the strategy we utilize in this work provides for another effective pathway to grow polymer brush films in a short time. Compared to solution (bulk) ROMP reactions which often complete within minutes, the brush growth kinetics is much slower by several orders of magnitude. And this effect is amplified by introducing more bulky functional groups in the norbornene pendants. In all the four cases listed in Figure 6, by increasing the number of the substituted terminal olefins, the polymer film thickness increases faster and approaches the constant equilibrium value earlier. This provides a strong proof that the density of the available alkenes for catalyst activation and film growth can be controlled. Furthermore, growth kinetics of the polynorbornene brush seemed to be very comparable regardless of the CV cycles, indicating that the density of the active olefins on the electropolymerized films from the same dendron molecules are not much different.

4. Conclusions

In this work, a series of peripheral olefin dendrons with electropolymerizable terthiophene functional group at the focal point were successfully synthesized. Electrochemical polymerization of these dendron molecules onto conducting substrates enabled ultrathin films with free olefins available for catalyst activation/initiation. This opens up a new route to prepare polymer brushes which can be achieved on any type and shape of conducting surfaces. By varying dendron generation or the number of the olefinic substituent on the branching sides, the density of such olefins can be changed. Therefore, the controlled synthesis of polymer brushes in terms of chain length, grafting density, and growth kinetics can be achieved. Polynorbornene was chosen as the model brush polymer to demonstrate the utility of these dendrons as surface initiators. AFM, XPS, and growth kinetics measurements confirmed the effect of the dendron structures on the growth kinetics and film thickness of the polymer brushes. Future work can focus on the nature of the electrodeposited conjugated polymer and its electro-optical properties. Other monomers designs can also be explored.

Acknowledgment. The authors acknowledge funding from the NSF CBET-0854979, DMR-10-06776, CHE-10-41300, Robert A. Welch Foundation E-1551, and the Texas NHARP 01846. Technical support from Agilent Technologies (Molecular Imaging), Malvern Instruments (Viscotek), and Optrel GmbH is also acknowledged.

Supporting Information Available: AFM images of the electrodeposited polythiophene films and the grafted polynorbornene brushes including summary of feature dimensions; electrochemical CV data on second-generation dendrons. This material is available free of charge via the Internet at http://pubs.acs.org.

References and Notes

(1) Advincula, R.; Ruehe, J.; Brittain, W.; Caster, K. E. *Polymer Brushes: On the Way to Tailor-Made Surfaces*, 1st ed.; Wiley-VCH: New York, 2004; pp 1−501.

(2) (a) Husseman, M.; Malmstrom, E. E.; McNamara, M.; Mate, M.; Mecerreyes, D.; Benoit, D. G.; Hedrick, J. L.; Mansky, P.; Huang, E.; Russell, T. P.; Hawker, C. J. *Macromolecules* **1999**, *32*, 1424–1431. (b) Kamigaito, M.; Ando, T.; Sawamoto, M. *Chem. Rev.* **2001**, *101*, 3689–3745. (c) Advincula, R. C. *J. Dispersion Sci. Technol.* **2003**, *24*, 343–361. (c) Edmondson, S.; Osborne, V. L.; Huck, W. T. S. *Chem. Soc. Rev.* **2004**, *33*, 14–22. (d) Tsujii, Y.; Ohno, K.; Yamamoto, S.; Goto, A.; Fukuda, T. *Adv. Polym. Sci.* **2006**, *197*, 1–45.

(3) (a) Kim, N. Y.; Jeon, N. L.; Choi, I. S.; Takami, S.; Harada, Y.; Finnie, K. R.; Girolami, G. S.; Nuzzo, R. G.; Whitesides, G. M.; Laibinis, P. E. *Macromolecules* **2000**, *33*, 2793–2795. (b) Rutenberg, I. M.; Scherman, O. A.; Grubbs, R. H.; Jiang, W.; Garfunkel, E.; Bao, Z. *J. Am. Chem. Soc.* **2004**, *126*, 4062–4063.

(4) Berron, B. J.; Graybill, E. P.; Jennings, G. K. *Langmuir* **2007**, *23*, 11651–11655.

(5) Samanta, S.; Locklin, J. *Langmuir* **2008**, *24*, 9558–9565.

(6) Kong, B.; Lee, J. K.; Choi, I. S. *Langmuir* **2007**, *23*, 6761–6765.

(7) Kurzawa, C.; Hengstenberg, A.; Schuhmann, W. *Anal. Chem.* **2002**, *74*, 355–361.

(8) Baute, N.; Teyssié, P.; Martinot, L.; Mertens, M.; Dubois, P.; Jérôme, R. *Eur. J. Inorg. Chem.* **1998**, 1711–1720.

(9) Baute, N.; Martinot, L.; Jérôme, R. *J. Electroanal. Chem.* **1999**, *472*, 83–90.

(10) Baute, N.; Jérôme, C.; Martinot, L.; Mertens, M.; Geskin, V. M.; Lazzaroni, R.; Brédas, J. L.; Jérôme, R. *Eur. J. Inorg. Chem.* **2001**, 1097–1107.

(11) Yildiz, G.; Çatalgil-Giz, H.; Kadirgan, F. *J. Appl. Electrochem.* **2000**, *30*, 71–75.

(12) Reuber, J.; Reinhardt, H.; Johannsmann, D. *Langmuir* **2006**, *22*, 3362–3367.

(13) Deniau, G.; Charlier, J.; Alvado, B.; Palacin, S.; Aplincourt, P.; Bauvais, C. *J. Electroanal. Chem.* **2006**, *586*, 62–71.

(14) Detrembleur, C.; Jérôme, C.; Claes, M.; Louette, P.; Jérôme, R. *Angew. Chem., Int. Ed.* **2001**, *40*, 1268–1271.

(15) Tria, M. C. R.; Grande, C. D. T.; Ponnapati, R.; Advincula, R. C. *Biomacromolecules* **2010**, Article ASAP.

(16) Xia, C. J.; Advincula, R. C. *Chem. Mater.* **2001**, *13*, 1682–1691.

(17) Taranekar, P.; Huang, C.; Fulghum, T. M.; Baba, A.; Jiang, G.; Park, J. Y.; Advincula, R. C. *Adv. Mater.* **2008**, *18*, 347–354.

(18) Taranekar, P.; Fulghum, T.; Patton, D.; Ponnapati, R.; Clyde, G.; Advincula, R. *J. Am. Chem. Soc.* **2007**, *129*, 12537–12548.

(19) Taranekar, P.; Fulghum, T.; Baba, A.; Patton, D.; Advincula, R. *Langmuir* **2007**, *23*, 908–917.

(20) Wendland, M. S.; Zimmerman, S. C. *J. Am. Chem. Soc.* **1999**, *121*, 1389–1390.

(21) Zimmerman, S. C.; Wendland, M. S.; Rakow, N. A.; Zharov, I.; Suslick, K. S. *Nature* **2002**, *418*, 399–403.

(22) Zimmerman, S. C.; Zharov, I.; Wendland, M. S.; Rakow, N. A.; Suslick, K. S. *J. Am. Chem. Soc.* **2003**, *125*, 13504–13518.

(23) Mertz, E.; Zimmerman, S. C. *J. Am. Chem. Soc.* **2003**, *125*, 3424–3425.

(24) Shon, Y. K.; Choi, D.; Dare, J.; Dinh, Tu. *Langmuir* **2008**, *24*, 6924–6931.

(25) Noda, T.; Shirota, Y. *J. Am. Chem. Soc.* **1998**, *120*, 9714–9715.

(26) Graf, D. D.; Duan, R. G.; Campbell, J. P.; Miller, L. L.; Mann, K. R. *J. Am. Chem. Soc.* **1997**, *1190*, 5888–5891.

(27) Jang, S. Y.; Marquez, M.; Sotzing, G. A. *J. Am. Chem. Soc.* **2004**, *126*, 9476–9477.

(28) Jang, S. Y.; Sotzing, G. A.; Marquez, M. *Macromolecules* **2002**, *35*, 7293–7300.

(29) Zotti, G.; Schiavon, G. *Synth. Met.* **1989**, *31*, 347–355.

(30) Smith, J. R.; Campbell, S. A.; Ratcliffe, N. M.; Dunleavy, M. *Synth. Met.* **1994**, *63*, 233–243.

(31) (a) Collis, G. E.; Burrell, A. K.; Scott, S. M.; Officer, D. L. *J. Org. Chem.* **2003**, *68*, 8974–8983. (b) Cutler, C. A.; Burrell, A. K.; Officer, D. L.; Too, C. O.; Wallace, G. G. *Synth. Met.* **2001**, *128*, 35–42.

(32) Rutenberg, I. M. *Functionalized Polymers and Surfaces via Ring-Opening Metathesis Polymerization*; California Institute of Technology: Pasadena, CA, 2005; pp 1−134.

(33) (a) Weck, M.; Jackiw, J. J.; Rossi, R. R.; Weiss, P. S.; Grubbs, R. H. *J. Am. Chem. Soc.* **1999**, *121*, 4088–4089. (b) Harada, Y.; Girolami, G. S.; Nuzzo, R. G. *Langmuir* **2003**, *19*, 5104–5114.

(34) Juang, A.; Scherman, O. A.; Grubbs, R. H.; Lewis, N. S. *Langmuir* **2001**, *17*, 1321–1323.

(35) Fulghum, T. M.; Patton, D. L.; Advincula, R. C. *Langmuir* **2006**, *22*, 8397–8402.

(36) Edmondson, S.; Vo, C.-D.; Armes, S. P.; Unali, G.-F.; Weir, M. P. *Langmuir* **2008**, *24*, 7208–7215.

(37) Fulghum, T. M.; Estillore, N. C.; Vo, C.-D.; Armes, S. P.; Advincula, R. C. *Macromolecules* **2008**, *41*, 429–435.

(38) Ostaci, R.-V.; Damiron, D.; Grohens, Y.; Leger, L.; Drockenmuller, E. *Langmuir* **2010**, *26*, 1304–1310.